

# Fluid-loaded metasurfaces

E. A. Skelton, R. V. Craster, and A. Colombi

*Department of Mathematics, Imperial College London, London, SW7 2AZ, U.K.*

D. J. Colquitt

*Department of Mathematical Sciences, University of Liverpool, Liverpool, L69 7ZL, U.K.*

(Dated: March 2, 2022)

We consider wave propagation along fluid-loaded structures which take the form of an elastic plate augmented by an array of resonators forming a metasurface, that is, a surface structured with sub-wavelength resonators. Such surfaces have had considerable recent success for the control of wave propagation in electromagnetism and acoustics, by combining the vision of sub-wavelength wave manipulation, with the design, fabrication and size advantages associated with surface excitation. We explore one aspect of recent interest in this field: graded metasurfaces, but within the context of fluid-loaded structures.

Graded metasurfaces allow for selective spatial frequency separation and are often referred to as exhibiting rainbow trapping. Experiments, and theory, have been developed for acoustic, electromagnetic, and even elastic, rainbow devices but this has not been approached for fluid-loaded structures that support surface waves coupled with the acoustic field in a bulk fluid. This surface wave, coupled with the fluid, can be used to create an additional effect by designing a metasurface to mode convert from surface to bulk waves. We demonstrate that sub-wavelength control is possible and that one can create both rainbow trapping and mode conversion phenomena for a fluid-loaded elastic plate model.

PACS numbers: PACS: 40.Rj, 40.Fz, 43.40.Dx, 43.40.Rj, 63.20.D-

## I. INTRODUCTION

The interaction of sound with compliant structures is a rich area of research that has generated significant interest, academic and otherwise, over the years with, at least, five monographs [1–5] on the subject. The interaction between acoustical and structural waves covers a very broad range of topics, with an equally broad range of techniques; from formal mathematical analyses (see, for example, [5]) to more applied research concerned with submarine acoustics [6]. In terms of physical problems, there are obvious applications, such as the generation of noise by flows past elastic structures (see, for example, [7]), flow in pipes [8], scattering of water waves by flexible ice sheets [9, 10], and the insonification of underwater elastic shells [11] amongst many others. The field itself has an illustrious history: The overview of the influence of fluid-loading on vibrating structures provided by Crighton’s 1998 Rayleigh Medal lecture [12] notes that it is almost impossible to find an area of research in wave motion where Lord Rayleigh has not worked and that fluid-loaded structures are no exception: In particular, Lord Rayleigh analysed the behaviour of air when excited by a vibrating circular plate [13] and his contemporaries, such as Lamb, also investigated similar problems [14].

Our interest here stems from recent advances in so-called metamaterials [15, 16] that are man-made composite structures that owe their properties to sub-wavelength structuration. These metamaterials can be designed to have effective properties not found in nature such as negative refractive index [17, 18] and these ideas which have proved highly effective in other areas of wave physics, primarily in electromagnetism [19], in terms of controlling wave motion but which are now influencing emergent areas such as acoustic [20, 21] and seismic [22–24] metamaterials. It is natural therefore to turn to fluid-loaded structures and evaluate whether metamaterials can be employed to any effect in this area. Since the structural acoustics of fluid-loading is inherently connected with a compliant surface such as an elastic plate or shell it is natural to consider metasurfaces rather than bulk metamaterials in this context.

An active area of research in metasurfaces [25] focusses upon graded resonator metasurfaces, where the general concept is that for a graded surface, or waveguide, different wavelengths are trapped at different spatial positions. Sub-wavelength microstructures are commonly employed in two ways. The first approach is to create effective macroscopic wavespeeds that vary spatially, thus achieving the required control of wave propagation. The second approach involves using deep sub-wavelength resonances to obtain the desired effects. Whilst the latter approach is significantly more difficult to create, it is far more powerful; hence our aim in the present paper is to extend this concept to fluid-loaded compliant structures. These ideas are being widely adopted in photonics and phononics due to their excellent abilities to control, manipulate and filter waves in compact devices. Graded and chirped designs include: trapping in rainbow devices [26, 27], flat focussing mirrors and lenses in optics, plasmonics and acoustics [28–33], gradient index lens for acoustic and flexural waves focussing [34, 35], acoustic absorbers [36, 37] and sound enhancement [38].

In the absence of the fluid-loading, it is only very recently that graded sub-wavelength structures for thin elastic plates has been considered as a chirped graded array [39], thin beams [40] or in the context of gradient index (GRIN) lenses created by graded structuration to control elastic symmetric ( $S_0$ ) and antisymmetric ( $A_0$ ) waves [41] and to obtain deeply sub-wavelength focussing [42], cloaking [43] and GRIN lenses (e.g. Luneburg, Maxwell-fisheye and Eaton lenses [40, 44]) using resonator arrays [35].

These are all primarily for effectively scalar wave systems and do not have the degrees of freedom necessary to demonstrate mode conversion from surface to bulk waves and so can only demonstrate trapped rainbow phenomena. More recently arrays of resonators atop elastic half-spaces have demonstrated, theoretically, numerically [23, 24] and experimentally in ultrasonics [45], that one can generate rainbow trapping phenomena and additionally manipulate surface Rayleigh waves and mode convert between Rayleigh and bulk shear waves. This mode conversion creates a surface device that is simultaneously reflectionless, yet has zero transmission into surface waves, and moreover that this occurs over an ultra-broadband range of frequencies. The rainbow trapping also has important implications as one can strongly enhance the surface wave amplitude at particular points along the interface and this is selectively achieved by altering the frequency.

The ability in elasticity to selectively use sub-wavelength graded resonator systems to influence both surface and bulk waves, as well as the coupling between them, motivates us to consider fluid-loaded structures. Although the governing equations are scalar, there is a coupling between the elastic waves in the plate and the acoustic pressure field in the fluid; it is this coupling that allows the structure to support a subsonic surface wave in addition to the bulk acoustic wave. We begin, in section II, by assessing the influence of attaching periodically arranged identical resonators, modelled by the simplest system, that of a mass-spring, to the fluid-loaded structure (as shown in Fig. 1). Scattering and radiation by periodic systems in the fluid-loaded literature are natural models of ribbed and reinforced structures such as a ship’s hull and have been much studied [46–51] amongst many others, and these analyses can be adapted to incorporate the resonator array. We deduce the dispersion relations that characterise the behaviour of waves within this periodic fluid-loaded plate- resonator system. These are utilised in section III to interpret the influence of grading the resonators by, for instance, increasing or decreasing the masses spatially along the array (as shown in Fig. 2) and this interpretation is complemented by careful numerical simulations for an incoming

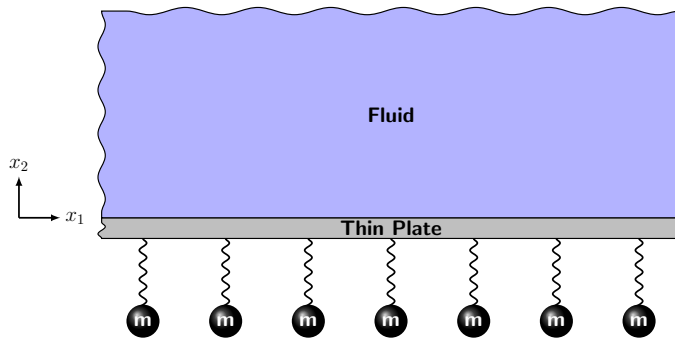


FIG. 1. A fluid-loaded elastic plate augmented by a periodic array of identical mass-spring resonators.

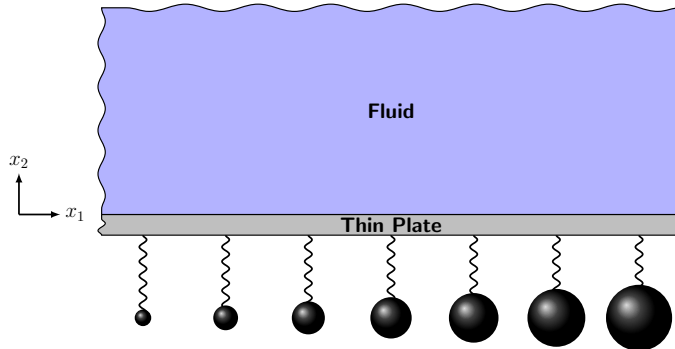


FIG. 2. A fluid-loaded elastic plate augmented by a periodic array of graded mass-spring resonators.

subsonic surface plate wave incident upon graded arrays. Given the interest in underwater acoustics and maritime structures we choose our numerical examples to have aluminium as the plate (thickness  $h = 0.01$  m, Young's modulus  $E_p = 69 \times 10^9$  N/m<sup>2</sup>, Poisson ratio  $\nu_p = 0.334$  and density  $\rho_p = 2700$  kg/m<sup>3</sup>) and water (density  $\rho_f = 1000$  kg/m<sup>3</sup>, and sound speed  $c_f = 1500$  m/s) as the fluid. Finally, we draw together some comments and future perspectives on the use of metamaterial ideas for fluid-loaded structures.

## II. FLUID-LOADED THIN ELASTIC PLATE - RESONATOR ARRAYS

### A. Formulation

We consider a thin elastic plate governed by the Kirchhoff-Love plate equations, as the simplest model of an elastic plate that captures the relevant physics for underwater acoustics [4] whilst recognising that this model can be complexified to allow the plate to be either anisotropic or thicker such that, say, the Mindlin equations become relevant; these generalisations are readily incorporated. We also restrict our attention to two-dimensions for clarity and as it will allow us to illustrate the key concepts without being over-burdened by excessive algebra.

Here, a thin elastic plate of thickness  $h$ , density  $\rho_p$ , Young's modulus  $E_p$  and Poisson's ratio  $\nu_p$  is located at  $z = 0$ ,  $-\infty < x < \infty$ . It is bounded on its upper surface by an infinite acoustic fluid ( $-\infty < x < \infty$ ,  $0 < z < \infty$ ) of density  $\rho_f$  and sound speed  $c_f$ . An infinite periodic array of mass-spring systems are attached to the lower surface of the plate, exerting point reaction forces, as shown in Fig. 1.

The (2D) equation of motion for a thin fluid-loaded plate is written as

$$D \frac{\partial^4}{\partial x^4} u(x, t) + M \frac{\partial^2}{\partial t^2} u(x, t) = \sum_{n=-\infty}^{\infty} F_n \delta(x - nd) - p(x, 0, t), \quad (1)$$

in which  $D = E_p h^3 / 12(1 - \nu_p^2)$  is the plate bending stiffness, and  $M = \rho_p h$ ,  $u(x, t)$  is the plate displacement,  $p(x, z, t)$  is the acoustic pressure in the fluid [4] and  $F_n$  is the reaction force of the  $n$ 'th mass-spring system located at  $x_n = nd$ .

The equation satisfied by the pressure in the acoustic fluid, with sound speed  $c_f$ , is the wave equation

$$\left( \frac{\partial^2}{\partial x^2} + \frac{\partial^2}{\partial z^2} - \frac{1}{c_f^2} \frac{\partial^2}{\partial t^2} \right) p(x, z, t) = 0, \quad (2)$$

with the continuity condition at the plate surface such that the normal velocity in the fluid there is equal to the normal velocity of the plate. The reaction forces  $F_n$  are determined from the equations of motion of the mass-spring system:

$$F_n = -m \frac{d^2}{dt^2} u_{mn}(t), \quad (3)$$

$$F_n = \lambda(u_{mn}(t) - u(nd, t)), \quad (4)$$

where  $m$  is the mass,  $\lambda$  is the spring constant and  $u_{mn}$  is the displacement of the attached mass at position  $x_n = nd$ .

### B. Dispersion relation

It is convenient to first consider time-harmonic motion, in which all the dependent variables are proportional to  $\exp(-i\omega t)$  and henceforth this exponential factor is suppressed. Thus, equations (1)–(4) become

$$D \frac{\partial^4}{\partial x^4} u(x) - M\omega^2 u(x) = \sum_{n=-\infty}^{\infty} F_n \delta(x - nd) - p(x, 0), \quad (5)$$

$$0 = \left( \frac{\partial^2}{\partial x^2} + \frac{\partial^2}{\partial z^2} + k^2 \right) p(x, z), \quad (6)$$

$$F_n = m\omega^2 u_{mn}, \quad (7)$$

$$F_n = \lambda(u_{mn} - u(nd)). \quad (8)$$

with  $k = \omega/c_f$  being the fluid wavenumber. Eliminating the mass displacements from (7) and (8) gives

$$F_n = -m\omega^2 \lambda u(nd) / (m\omega^2 - \lambda) = -L(\omega) u(nd). \quad (9)$$

For the mass-spring system here  $L(\omega) = m\omega^2 \lambda / (m\omega^2 - \lambda)$  and resonance occurs at  $\omega = \sqrt{\lambda/m}$ ; more complicated arrangements of masses and springs, or rods, can be considered leading to more complex functions encapsulated within  $L(\omega)$ . Fourier transform pairs for the plate displacement and the acoustic pressure are introduced, for example, for the plate displacement:

$$u(x) = \frac{1}{2\pi} \int_{-\infty}^{\infty} \bar{u}(\alpha) \exp(i\alpha x) d\alpha, \quad (10)$$

$$\bar{u}(\alpha) = \int_{-\infty}^{\infty} u(x) \exp(-i\alpha x) dx. \quad (11)$$

Transforming (10) we see the pressure is

$$\bar{p}(\alpha, z) = \bar{p}(\alpha, 0) e^{i\gamma z} \quad (12)$$

where  $\gamma = \sqrt{k^2 - \alpha^2}$  and the continuity condition at the plate surface couples the pressure to the plate displacement and

$$i\gamma \bar{p}(\alpha, 0) = \rho\omega^2 \bar{u}(\alpha). \quad (13)$$

Making use of the Poisson Summation Formula [52], the reaction force terms of equation (5) can be written in the

form

$$\sum_{n=-\infty}^{\infty} F_n \delta(x - nd) = \frac{-L(\omega)}{d} u(x) \sum_{n=-\infty}^{\infty} \exp(2\pi i n x / d), \quad (14)$$

from which the transformed Eq. (5) becomes

$$S(\alpha, \omega) \bar{u}(\alpha) + \frac{L(\omega)}{d} \sum_{n=-\infty}^{\infty} \bar{u}(\alpha - 2n\pi/d) = 0, \quad (15)$$

where  $S(\alpha, \omega) = D\alpha^4 - \omega^2 M - i\rho\omega^2/\gamma$ .

In the absence of any forcing or resonators, that is if we consider a pristine elastic plate with fluid loading, the dispersion relation is given by  $S(\alpha, \omega) = 0$ . Going one level even simpler, that is to an elastic plate *in vacuo*  $D\alpha^4 - \omega^2 M = 0$  and  $\alpha = (M\omega^2/D)^{1/4}$  giving the flexural plate wavenumber-frequency relationship that is nonlinear and which indicates that these plate waves are dispersive. The addition of the fluid coupling leads to these flexural plate waves acquiring a complex component and they become leaky waves, and we shall not consider them further here. The fluid-loaded system also allows for a subsonic (relative to the overlying fluid) surface wave that exists due to the coupling between the fluid and plate and which exponentially decays into the fluid. This wave is effectively the primary excitation of the arrays we describe and our aim is to investigate how this surface wave interacts with the resonant array.

Returning to the array of resonators, Eq. (15) becomes

$$\left[ 1 + \frac{L(\omega)}{d} \sum_{n=-\infty}^{\infty} \frac{1}{S(\alpha - 2n\pi/d, \omega)} \right] \sum_{n=-\infty}^{\infty} \bar{u}(\alpha - 2n\pi/d) = 0 \quad (16)$$

and the dispersion relation for the periodic system is therefore

$$1 + \frac{L(\omega)}{d} \sum_{n=-\infty}^{\infty} \frac{1}{S(\alpha - 2n\pi/d, \omega)} = 0. \quad (17)$$

There are limits of (17) that are of interest and which can be approached analytically. For no fluid-loading the infinite sum of (17) can be evaluated exactly, as in for example [24], allowing a closed form expression for the dispersion relation. With fluid present in the upper half-space the situation is more complicated and a closed form expression appears unavailable. Leading order asymptotic approximations for sums of this form are available [49] in the heavy fluid-loading limit for which  $\tilde{\alpha}_1 \gg k$ , and  $\tilde{\alpha}_1 \gg \tilde{\alpha}_0$ ,

$$\sum_{n=-\infty}^{\infty} \frac{1}{S(\alpha - 2n\pi/d, \omega)} \sim \frac{-d}{5D\tilde{\alpha}_1^3} \left\{ \cot\left(\frac{2\pi}{5}\right) + \frac{\sin(\tilde{\alpha}_1 d)}{\cos(\alpha d) - \cos(\tilde{\alpha}_1 d)} \right\}, \quad (18)$$

in which  $\tilde{\alpha}_1 = (\rho\omega^2/D)^{1/5}$  is the wavenumber in the heavily fluid-loaded plate and  $\tilde{\alpha}_0 = (\omega^2 M/D)^{1/4}$ , the wavenumber of the *in vacuo* plate. Hence, in this heavy fluid-loading approximation, we rewrite  $\alpha$  as a function of  $\omega$  as

$$\cos(\alpha d) = \cos(\tilde{\alpha}_1 d) + \frac{\sin(\tilde{\alpha}_1 d)}{\frac{5D\tilde{\alpha}_1^3}{L(\omega)} - \cot\left(\frac{2\pi}{5}\right)}. \quad (19)$$

From this expression, for a given value of  $\omega$ , real values of  $\alpha$  are only obtained when the absolute value of the right hand side of (19) is less than or equal to 1. Numerical examination of this dispersion relation shows that in this low frequency, heavy fluid-loading, asymptotic regime the dispersion diagram does not exhibit the band gaps necessary to provide interesting metamaterial properties. Thus, we proceed to investigate the full dispersion relation, away from the aforementioned asymptotic limits, numerically.

Returning to (17), and writing it as

$$\sum_{n=-\infty}^{\infty} \frac{1}{S(\alpha_n, \omega)} = \frac{-d}{L(\omega)} \quad (20)$$

in which  $\alpha_n = \alpha - 2n\pi/d$ , we note that the right hand side is always real, whereas the left hand side will have an

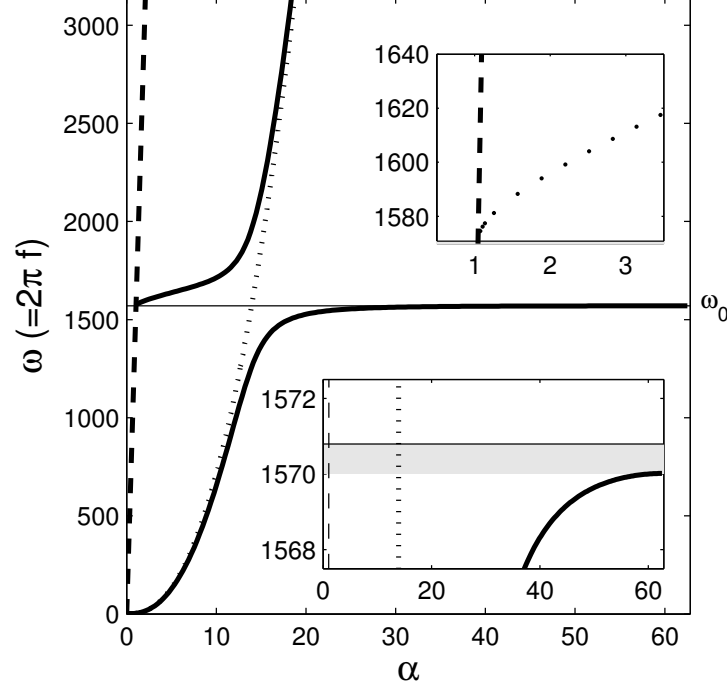


FIG. 3. Dispersion plot showing frequency  $\omega = 2\pi f$  as a function of horizontal wavenumber  $\alpha$  (solid black lines) for 1 cm aluminium plate in water and periodic mass-spring resonators with spacing  $d = 5$  cm. Range for  $\alpha$  is  $[0, \pi/d]$ . Asymptotes shown: dashed line is  $\alpha = \omega/c_f$  (sound line), dotted line is unconstrained fluid-loaded plate dispersion plot showing  $\tilde{\alpha}_1$ , solid black line is resonance frequency of resonators. Insets show zoom-in on very narrow band gap (shaded grey), and zoom-in on the asymptote to the sound line.

imaginary part unless  $\gamma_n = \sqrt{k^2 - \alpha_n^2}$  is imaginary for each value of  $n$ . Thus, for any given value of  $\omega$ , this restricts the possible values of  $\alpha$ :  $k < \alpha < 2\pi/d - k$  when  $0 < \alpha < 2\pi/d$  and  $0 < k < \pi/d$ .

Due to the underlying periodicity, the dispersion diagram repeats in  $\alpha$  with period  $2\pi/d$ . To find the roots we note that for any given value of  $\omega$ ,  $S(\alpha, \omega)$  has one real positive root and therefore,  $1/S(\alpha, \omega)$  passes through an infinity there and changes sign. Thus, the left hand side of (20), as a function of  $\alpha$ , periodically varies from  $-\infty$  to  $\infty$  and must therefore equal the right hand side at least once in each such interval. For heavy fluid loading such solutions are close to the location of the infinities, but are found numerically by starting the searches very close to the location of the infinity (where the sign is known) and looking for a change of sign.

We choose typical parameters in Fig. 3 that shows the fluid-loaded plate - resonator curves together with the resonator frequency ( $\omega_0$ ), the acoustic sound line  $\omega = \alpha c_f$  (dashed line) and the sub-sonic coupled fluid-plate surface wave (dotted line). The effect of the resonator is to punch through the surface wave mode to create a very narrow band gap, shown as the gray region in the inset to Fig. 3, and the hybridisation of the mode. The hybridisation shows a transition, as one decreases frequency and approach the band gap from above, in behaviour from the coupled fluid-solid surface wave to the bulk acoustic mode. This behaviour, arising from the avoided crossing between the surface wave dispersion relation and the local resonance is the acoustic manifestation of a surface plasmon polariton [53] in condensed matter physics which is one of the main approaches in nanofabricated devices used to design and control the propagation of light. A key difference in this fluid-loaded analogy is that the mode below resonance emerges from a surface wave that is dispersive and so the analogy is not exact.

For typical underwater parameters the band-gap thickness remains narrow over a wide range of frequencies and resonator mass, see Fig. 4, and such a narrow frequency band suggests that the effect of the band-gap will be only restricted to very limited frequencies and be of little use. This is relatively common in graded resonator systems, the resonating rods atop an elastic surface interacting with surface Rayleigh waves [24] have similar behaviour, and to take advantage of the band-gap the key addition is to make the resonant array spatially dependent in some way. The spatial dependence can come through a gradual change in the array spacing, a graduation of spring constant or mass in each resonator along the array. We choose to alter the masses in the array by either linearly ramping them up, or down, with distance and illustrate how this influences an incident surface wave coming from a pristine region of the

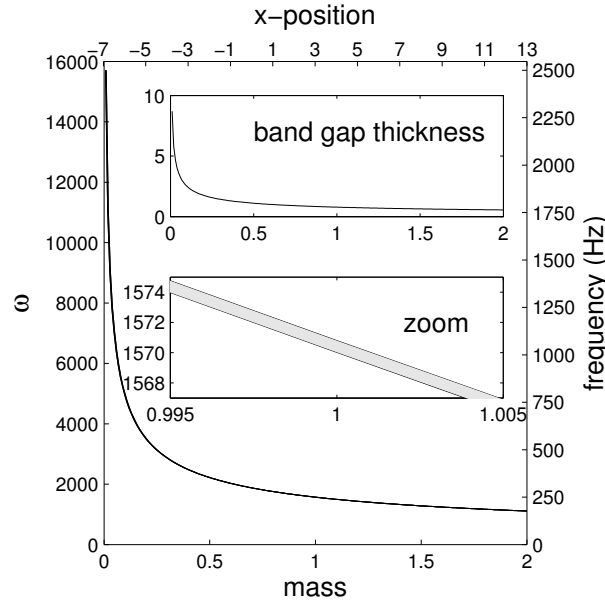


FIG. 4. Frequency band gap as a function of resonator mass for identical periodically spaced resonators. The upper limit of the band gap is the resonance frequency of the mass-spring system. The band gap too narrow to be observable on this scale. The lower inset shows a zoom in of the main plot with the shaded area the band gap. The upper inset shows, as a line plot, the band gap width as a function of mass.

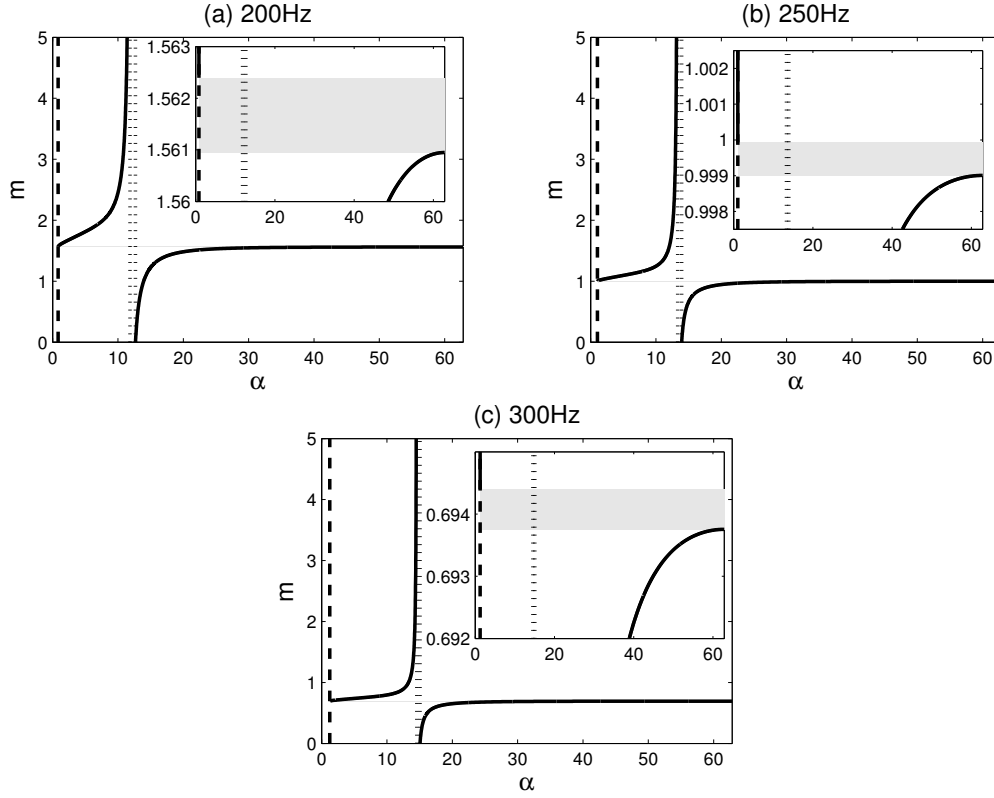


FIG. 5. For fixed frequencies (200, 250 and 300 Hz from top to bottom), spring constant and spacing dispersion plot showing mass as a function of horizontal wavenumber for 1 cm aluminium plate in water. Asymptotes shown: dashed line is  $\alpha = \omega/c_f$  (sound line), solid line is obtained numerically, dotted line is the wavenumber of the unconstrained fluid-loaded plate. Inset shows zoom-in on very narrow band gap (shaded grey).

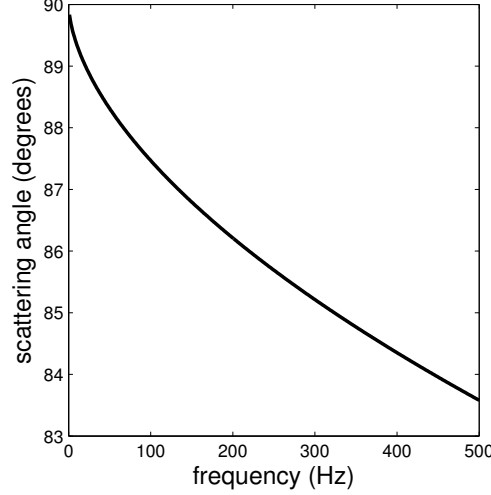


FIG. 6. The variation of scattering angle with frequency.

plate not containing resonators striking a semi-infinite array of resonators. The choice of mass change with position mean that the horizontal axis is equivalently the  $x$ -position of the resonators and we note that for a mass of 1 kg the position is 3 m and the frequency is 250 Hz and these choices are used later. Fig. 4 allows us to read off the position,  $x = (\lambda/\omega^2 - m(0))/(dm/dx)$ , as a function of  $m(x)$ , at which waves are no longer supported by the array as a function of position and thus this curve gives the turning point and thus shows the spatial selection by frequency.

### C. Graded array

The conventional dispersion diagram of Fig. 3 for frequency versus wavenumber comes from Eq. (17), with  $L(\omega)$  defined in (9) and all parameters (plate and fluid properties, mass-spring properties and the spacing) remaining constant. An alternative, less common, but instructive diagram are those of Fig. 5 that considers how the modes vary with a parameter, but now holding frequency fixed. As frequency decreases, from top to bottom, in Fig. 5, one sees the bandgap move downwards as predicted by Fig. 4 and the vertical asymptote more to the right, that is, to shorter waves. Fig. 5 gives a valuable interpretation, for graded structures, as one can follow a branch from, say, high mass to low mass or vice-versa, and then immediately see how the wave system behaves. Before embarking upon this interpretation we extract the exact mass-frequency relationship.

The mass and spring constants only enter into (17) via the  $L(\omega)$  term, and the dispersion relation can be re-written as

$$\frac{\omega^2 - \lambda/m}{\omega^2 \lambda} = \frac{-1}{d} \sum_{n=-\infty}^{\infty} \frac{1}{S(\alpha - 2n\pi/d, \omega)}. \quad (21)$$

Hence, if  $\omega$  and  $\lambda$  are held constant, then the relation between resonator mass  $m$  and wavenumber  $\alpha$  is explicit:

$$m = \frac{\lambda}{\omega^2 \left( 1 + \frac{\lambda}{d} \sum_{n=-\infty}^{\infty} \frac{1}{S(\alpha - 2n\pi/d, \omega)} \right)}, \quad (22)$$

and similarly, holding  $\omega$  and  $m$  constant, a relation between resonator spring constant  $\lambda$  and  $\alpha$  also emerges:

$$\lambda = \frac{\omega^2}{\left( \frac{1}{m} + \frac{\omega^2}{d} \sum_{n=-\infty}^{\infty} \frac{1}{S(\alpha - 2n\pi/d, \omega)} \right)}. \quad (23)$$

Plotting the mass versus wavenumber, using (22), in Fig. 5 allows us to predict and interpret the behaviour of



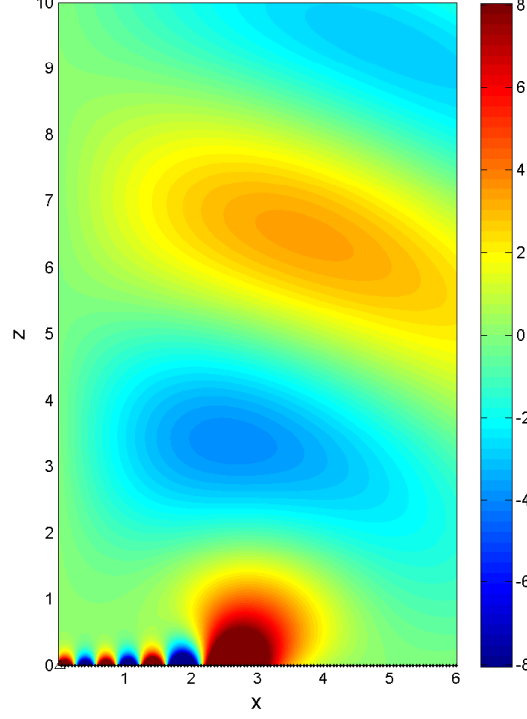


FIG. 7. Time-harmonic (250Hz) snapshot of pressure in water above 1 cm aluminium plate with mass-spring resonators. Resonator mass decreases with  $x$ . Resonant frequency of mass-spring located at  $x = 3$  is 250Hz.

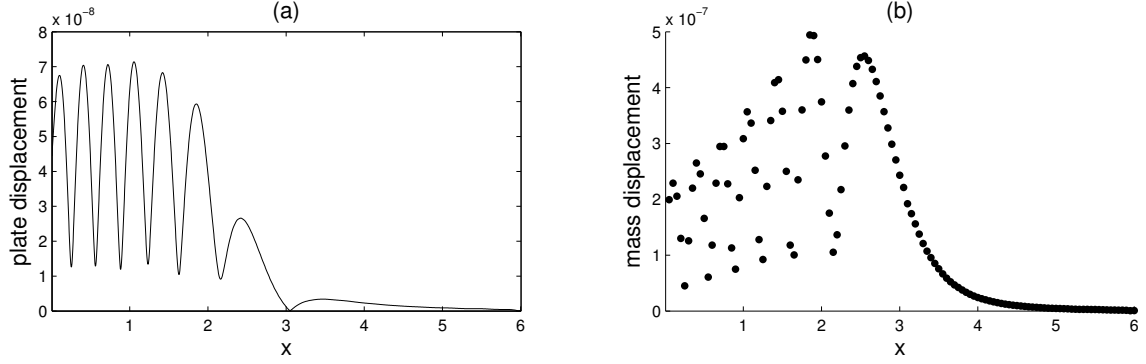


FIG. 8. Decreasing resonator mass: Time-harmonic (250 Hz) displacements of 1cm aluminium plate with water-loading and mass-spring resonators with the resonant frequency of mass-spring located at  $x = 3$  at 250 Hz. The absolute values of the plate and mass displacements are shown in the top and bottom panels respectively.

waves associated with a plate with an array of mass-spring resonators for which the spacing and spring constant are held constant, but the mass of the resonators varies (smoothly and monotonically) with position.

We first consider what happens to a wave as it moves through an array of gradually decreasing masses, i.e. ramping down the mass. From Fig. 5 for fixed frequency we start from the top of the graph and follow the dispersion curve downwards. Initially the surface wave propagates there with a horizontal wavenumber in the plate close to that of the surface wave in a pristine plate, and in the fluid with corresponding exponential decay in the direction perpendicular to the plate; this is effectively the dashed line of Fig. 3. As the wave progresses through the array, it encounters ever smaller values of the resonator mass, and the wavenumber adapts by also decreasing c.f. Fig. 5 and the exponential rate of decay of the wave in the fluid perpendicular to the plate also decreases. The surface wave hybridises and moves towards the bulk acoustic wave branch until, for say 250 Hz at  $m \sim 1$ , the curve arrives at the band gap and meets

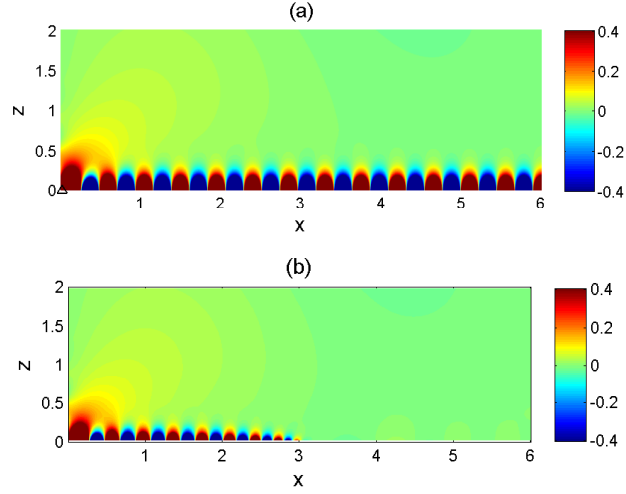


FIG. 9. Time-harmonic (250Hz) snapshot of pressure in water above 1cm aluminium plate: Top, a pristine plate without resonators and bottom, with mass-spring resonators. Resonator mass increases with  $x$ . Resonant frequency of mass-spring located at  $x = 3$  is 250Hz.

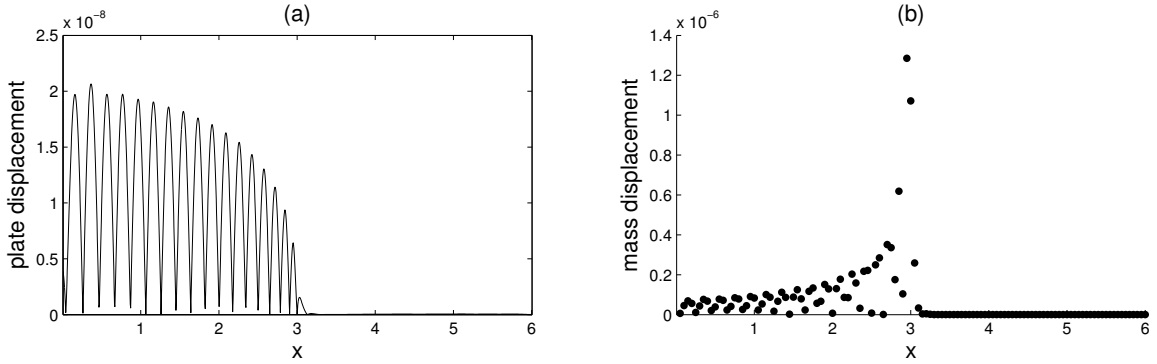


FIG. 10. Increasing resonator mass: Time-harmonic (250 Hz) displacements of 1cm aluminium plate with water-loading and mass-spring resonators with the resonant frequency of mass-spring located at  $x = 3$  at 250 Hz. The absolute values of the plate and mass displacements, are shown in the top and bottom panels respectively.

the acoustic branch. At this point the system can no longer support a wave propagating in the direction parallel to the plate as the resonator mass decreases further. However the energy within the surface wave has to go somewhere, and the energy contained in the wave must be radiated out into the fluid, the point at which this occurs can be explicitly predicted from Fig. 4. Thus we have constructed a situation where mode conversion from a surface wave to a bulk wave occurs and where, as far as the surface displacement is concerned, there is both vanishing reflection and transmission. The cosine of the angle at which waves leave the surface is simply given by the ratio of sound speeds, i.e.  $\cos \theta = (c_f/c_p)$ , and, as shown in, Fig. 6, and is verified from the numerical results.

If we now consider the contrasting case, that of ramping up the mass with a wave moving through an array of gradually increasing masses, that is we start from the lower branch of the curve, which cuts on at zero mass and  $\alpha = \alpha_1$ . As this wave progresses it encounters ever larger values of resonator mass and the wavenumber adapts and increases, until when  $\alpha = \pi/d$  the curve arrives at the lower edge of the band gap. However, at this point, because of the continuity of the curve there (due to symmetry and periodicity) the wave is totally reflected. This is the origin of so-called rainbow trapping as the position at which this reflection occurs is frequency dependent and so one can design selective spatial frequency separation of waves.

### III. NUMERICAL RESULTS

We now turn to numerical simulations to illustrate the mode conversion and rainbow trapping effects. The numerical simulations use the finite difference method together with perfectly matched layers (PML) [54, 55] which are used to mimic an infinite domain; this is done by surrounding a finite area of fluid, and the corresponding finite length of plate, with a finite thickness of PML. The forcing is taken to be at the origin and of form  $\delta(x)\exp(-i\omega t)$ . This is implemented in finite differences in the frequency domain with at least 10 grid points between each resonator to ensure sufficient resolution per wavelength.

We first consider the effect of ramping down the masses and the potential for mode conversion. We use 120 mass-spring resonators with spacing  $d = 0.05$  m and graduate the masses by linearly ramping them down from 1.3 kg to 0.705 kg in graduations of 0.005 kg. The spring constant  $\lambda$  is fixed as  $2.4674 \times 10^6$  kg  $\cdot$  s $^{-2}$  which is chosen to give a resonant freq of 250 Hz for  $m = 1$  kg. The mode conversion is strikingly seen in Fig. 7, which shows the surface wave propagating along the array with a gradually increasing wavelength, see Fig. 8, until it reaches the critical point, here  $x \sim 3$  m, where the surface wave mode has hybridised into a bulk wave and the energy radiates into the bulk as highly directional long waves; clearly the resonator spacing (of 0.05 m) is sub-wavelength and for comparison the wavelength for the unconstrained fluid-loaded plate is 0.4508 m and the wavelength in the fluid 6 m. This striking mode conversion is accompanied by decreasing plate and resonator displacements as the wave mode converts.

The rainbow trapping phenomena is illustrated in Fig. 9, and the masses now increase in amplitude. This figure also shows the wavefield in the absence of resonators as a reference for comparison with Figs. 7, as well as the varying masses case of Fig. 9. We again use 120 mass-spring resonators with spacing  $d = 0.05$  m and reverse the graduation with the masses linearly ramping up from 0.705 kg to 1.3 kg in increments of 0.005 kg and with the spring constant  $\lambda$  is fixed as  $2.4674 \times 10^6$  kg  $\cdot$  s $^{-2}$ . The surface wave has gradually decreasing amplitude as it passes through the array and gets cut-off at  $x \approx 3$ ; for different frequencies this position varies and this position can be read off directly from Fig. 4. Here we witness almost total reflection, and notably the plate surface displacement tends to zero, but the amplitude of the mass resonators increases dramatically, Fig. 10, thus the motion is spatially localised on the resonators which is ideal for applications such as energy harvesting.

### IV. DISCUSSION

We have illustrated that metamaterial ideas, that is using arrays of local sub-wavelength structuration to influence global wave behaviour, are relevant to fluid-loaded structures. We have concentrated upon a feature, surface graded arrays of resonators, pertinent to energy harvesting, structural vibration damping, mode conversion and the control of waves on surfaces. We envisage, as in the theory of surface elastic wave mode conversion and rainbow trapping [24] which prompted experimental verification [45], that the theory we present here will drive experimental work. In more general terms, it is clear that other features such as effective negative parameters, analogies of transformation optics and much more are transferable from metamaterials to the field of structural acoustics. It is also important to note that we have treated the simplest possible type of resonator, masses and springs, but the analysis easily generalises to more realistic rod-resonator arrays as utilised in, the non-fluid loaded plate, analyses of [24, 56].

We also remark that, in recent years, there has been significant interest in so-called *bifunctional metamaterials* which aim to harness the power of two different physical phenomena to achieve metamaterial effects. Thus far however, these approaches have focused on the control of fields that, fundamentally, are governed by the same physics and have the same underlying mathematical structure (see, for example, [57–60]); thermal and electrical conduction are both governed by the Helmholtz operator, for example. In contrast, the present paper represents a step change in the study of *bifunctional metamaterials*. Here we demonstrate a truly bifunctional metamaterial, synthesising two fundamentally different physical systems, acoustic fluid (governed by the Helmholtz operator) and flexural plate waves (governed by the biharmonic operator), to create the striking mode conversion illustrated in §II C.

We emphasise that, whilst motivated by the seismic metawedge [23, 24], the present work goes far beyond the mode conversion demonstrated by the metawedge. The elastic metawedge examined in [23, 24] is capable of converting elastic surface waves into elastic bulk waves, that is, conversion from one elastic mode to another. In contrast, the fluid-loaded metasurface is capable of converting flexural plate waves to acoustic waves, that is, converting mechanical waves into acoustic waves. In this sense, the fluid-loaded metasurface studied in the present paper transcends the boundaries between disparate physical phenomena creating a truly bifunctional metasurface.

## ACKNOWLEDGMENTS

This research was supported by the U.K. EPSRC under grant EP/L024926/1 and by a Marie-Curie Fellowship to AC.

## REFERENCES

- 
- [1] L. Cremer, M. Heckl, and B. A. T. Petersson, *Structure-borne sound: structural vibrations and sound radiation at audio frequencies* (Springer-Verlag, Berlin, 2004), 3 ed.
  - [2] F. J. Fahy and P. Gardonio, *Sound and structural vibration: radiation, transmission and response* (Academic press, London, 1987).
  - [3] E. A. Skelton and J. H. James, *Theoretical acoustics of underwater structures* (Imperial College Press, London, 1997).
  - [4] M. C. Junger and D. Feit, *Sound, structures, and their interaction* (MIT press, Cambridge, MA, 1972).
  - [5] D. Crighton, A. Dowling, J. Ffowcs-Williams, M. Heckl, and F. Leppington, *Modern Methods in analytical acoustics* (Springer-Verlag, Berlin, 1992).
  - [6] M. Caresta and N. J. Kessissoglou, “Acoustic signature of a submarine hull under harmonic excitation,” *Applied Acoustics* **71**, 17–31 (2010).
  - [7] M. S. Howe, “Rayleigh Lecture 2007: Flow-surface interaction noise,” *Journal of Sound and Vibration* **314**, 113–146 (2008).
  - [8] D. Yu, M. P. Païdoussis, H. Shen, and L. Wang, “Dynamic Stability of Periodic Pipes Conveying Fluid,” *Journal of Applied Mechanics* **81**, 011008 (2013).
  - [9] N. J. Balmforth and R. V. Craster, “Ocean waves and ice sheets,” *Journal of Fluid Mechanics* **395**, 89–124 (1999).
  - [10] R. Porter and D. V. Evans, “Diffraction of flexural waves by finite straight cracks in an elastic sheet over water,” *Journal of Fluids and Structures* **23**, 309–327 (2007).
  - [11] G. Gaunaurd and M. Werby, “Acoustic resonance scattering by submerged elastic shells,” *Applied Mechanics Reviews* **43**, 171–208 (1990).
  - [12] D. G. Crighton, “The 1988 Rayleigh Medal Lecture: Fluid Loading - The interaction between sound and vibration,” *Journal of Sound and Vibration* **133**, 1–27 (1989).
  - [13] J. W. Strutt, *The theory of sound* (MacMillan, New York, 1896).
  - [14] H. Lamb, “On the Vibrations of an Elastic Plate in Contact with Water,” *Proceedings of the Royal Society of London* **98**, 205–216 (1920).
  - [15] J. B. Pendry, A. J. Holden, D. J. Robbins, and W. J. Stewart, “Extremely low frequency plasmons in metallic mesostructures,” *Phys. Rev. Lett.* **76**, 4773–4776 (1996), doi:10.1103/PhysRevLett.76.4773.
  - [16] J. B. Pendry, A. J. Holden, W. J. Stewart, and I. Youngs, “Magnetism from conductors and enhanced nonlinear phenomena,” *IEEE Trans. Micr. Theo. Tech.* **47**, 2075 (1999).
  - [17] V. G. Veselago, “The Electrodynamics of substances with simultaneously negative values of  $\epsilon$  and  $\mu$ ,” *Soviet Physics Uspekhi* **10**, 509 (1968).
  - [18] J. B. Pendry, “Negative Refraction Makes a Perfect Lens,” *Phys. Rev. Lett.* **85**, 3966–3969 (2000).
  - [19] J. B. Pendry, D. Schurig, and D. R. Smith, “Controlling Electromagnetic Fields,” *Science* **312**, 1780–1782 (2006).
  - [20] Z. Liu, X. Zhang, Y. Mao, Y. Zhu, Z. Yang, C. Chan, and P. Sheng, “Locally Resonant Sonic Materials,” *Science* **289**, 1734–1736 (2000).
  - [21] R. Craster and S. Guenneau, *Acoustic Metamaterials: Negative Refraction, Imaging, Lensing and Cloaking* (London: Springer, 2012).
  - [22] S. Brûlé, E. H. Javelaud, S. Enoch, and S. Guenneau, “Experiments on seismic metamaterials: Molding surface waves,” *Phys. Rev. Lett.* **112**, 133901 (2014).
  - [23] A. Colombi, D. Colquitt, P. Roux, S. Guenneau, and R. V. Craster, “A seismic metamaterial: The resonant metawedge,” *Sci. Rep.* **6**, 27717 (2016).
  - [24] D. Colquitt, A. Colombi, R. Craster, P. Roux, and S. Guenneau, “Seismic metasurfaces: Sub-wavelength resonators and Rayleigh wave interaction,” *J. Mech. Phys. Solids* **99**, 379–393 (2017).
  - [25] A. A. Maradudin, *Structured Surfaces as Optical Metamaterials* (Cambridge University Press, 2011).
  - [26] K. L. Tsakmakidis, A. D. Boardman, and O. Hess, “Trapped rainbow storage of light in metamaterials,” *Nature* **450**, 397–401 (2007).
  - [27] M. Jang and H. Atwater, “Plasmonic rainbow trapping structures for light localization and spectrum splitting,” *Phys. Rev. Lett.* **107**, 207401 (2011).
  - [28] N. Yu and F. Capasso, “Flat optics with designer metasurfaces,” *Nature Materials* **13**, 139–149 (2014).
  - [29] L. Maigyte, V. Purlys, J. Trull, M. Peckus, C. Cojocar, D. Gailevicius, M. Malinauskas, and K. Staliunas, “Flat lensing in the visible frequency range by woodpile photonic crystals,” *Optics Letters* **38**, 2376–2378 (2013).

- [30] Y. Cheng, S. Kicas, J. Trull, M. Peckus, C. Cojocaru, R. Vilaseca, R. Drazdys, and K. Staliunas, “Flat focussing mirror,” *Sci. Rep.* **4**, 6326 (2014).
- [31] M. Kadic, S. Guenneau, S. Enoch, and S. Ramakrishna, “Plasmonic space folding: Focussing surface plasmons via negative refraction in complementary media,” *ACS Nano* **5**, 6819–6825 (2011).
- [32] J. Christensen and F. J. G. de Abajo, “Anisotropic metamaterials for full control of acoustic waves,” *Phys. Rev. Lett.* **108**, 124301 (2012).
- [33] N. Kundtz and D. R. Smith, “Extreme-angle broadband metamaterial lens,” *Nat. Mater* **9**, 129–132 (2010).
- [34] T. P. Martin, M. Nicholas, G. J. Orris, L.-W. Cai, D. Torrent, and J. Sanchez-Dehesa, “Sonic gradient index lens for aqueous applications,” *Appl. Phys. Lett.* **97**, 113503 (2010).
- [35] A. Colombi, “Resonant metalenses for flexural waves,” *J. Acoust. Soc. Am.* **140**, EL423 (2016).
- [36] J. Zhu, Y. Chen, X. Zhu, F. J. Garcia-Vidal, X. Yin, W. Zhang, and X. Zhang, “Acoustic rainbow trapping,” *Sci. Rep.* **3**, 1728 (2013).
- [37] N. Jimenez, V. Romero-Garcia, A. Cebrecos, R. Pico, V. J. Sanchez-Morcillo, and L. M. Garcia-Raffi, “Broadband quasi perfect absorption using chirped multi-layer porous materials,” *AIP Advances* **6**, 121605 (2016).
- [38] V. Romero-Garcia, R. Pico, A. Cebrecos, V. J. Sanchez-Morcillo, and K. Staliunas, “Enhancement of sound in chirped sonic crystals,” *Appl. Phys. Lett.* **102**, 091906 (2013).
- [39] Z. Tian and L. Yu, “Rainbow trapping of ultrasonic guided waves in chirped phononic crystal plates,” *Sci. Rep.* **7**, 40004 (2017).
- [40] D. Cardella, P. Celli, and S. Gonella, “Manipulating waves by distilling frequencies: a tunable shunt-enabled rainbow trap,” *Smart Materials and Structures* **25**, 085017 (2016).
- [41] Y. Jin, D. Torrent, Y. Pennec, Y. Pan, and B. Djafari-Rouhani, “Simultaneous control of the S0 and A0 Lamb modes by graded phononic crystal plates,” *J. Appl. Phys.* **117**, 244904 (2015).
- [42] A. Colombi, P. Roux, and M. Rupin, “Sub-wavelength energy trapping of elastic waves in a meta-material,” *J. Acoust. Soc. Am.* **136**, EL192–8 (2014).
- [43] A. Colombi, P. Roux, S. Guenneau, and M. Rupin, “Directional cloaking of flexural waves in a plate with a locally resonant metamaterial,” *J. Acoust. Soc. Am.* **137**, 1783–9 (2015).
- [44] M. H. Rudolf Karl Luneburg, *Mathematical Theory of Optics* (University of California Press, 1964), 1st edition.
- [45] A. Colombi, R. V. Craster, V. A. R. J. Smith, R. Patel, M. Clark, D. Colquitt, A. Clare, S. Guenneau, and P. Roux, “Enhanced sensing and conversion of ultrasonic Rayleigh waves by elastic metasurfaces,” <https://arxiv.org/abs/1704.01553>.
- [46] V. Evseev, “Sound radiation from an infinite plate with periodic inhomogeneities,” *Soviet Physics Acoustics* **19**, 226–229 (1973).
- [47] F. G. Leppington, “Acoustic Scattering by membranes and plates with line constraints,” *Journal of Sound and Vibration* **58**, 319–332 (1978).
- [48] B. Mace, “Periodically stiffened fluid-loaded plates, II: Response to line and point forces,” *Journal of Sound and Vibration* **73**, 487–504 (1980).
- [49] E. A. Skelton, “Acoustic Scattering by Parallel Plates with Periodic Connectors,” *Proceedings of the Royal Society A: Mathematical, Physical and Engineering Sciences* **427**, 419–444 (1990).
- [50] A. D. Pierce, V. W. Sparrow, and D. A. Russell, “Fundamental structural-acoustic idealizations for structures with fuzzy internals,” *J. Vib. Acoust.* **117**, 339–348 (1995).
- [51] R. L. Weaver, “Multiple-scattering theory for mean responses in a plate with sprung masses,” *The Journal of the Acoustical Society of America* **101**, 3466–3474 (1997).
- [52] A. Deitmar and S. Echterhoff, *Principles of harmonic analysis* (Springer, 2014).
- [53] A. Otto, “Excitation of nonradiative surface plasma waves in silver by the method of frustrated total reflection,” *Zeitschrift für Physik* **216**, 398–410 (1968).
- [54] J.-P. Berenger, “A perfectly matched layer for the absorption of electromagnetic waves,” *J. Comp. Phys.* 185–200 (1994).
- [55] E. A. Skelton, S. D. M. Adams, and R. V. Craster, “Guided elastic waves and perfectly matched layers,” *Wave Motion* **44**, 573–592 (2007).
- [56] E. G. Williams, P. Roux, M. Rupin, and W. A. Kuperman, “Theory of multiresonant metamaterials for  $A_0$  Lamb waves,” *Phys. Rev. B* **91**, 104307 (2015), URL <http://link.aps.org/doi/10.1103/PhysRevB.91.104307>.
- [57] T. J. Kippenberg and K. J. Vahala, “Cavity opto-mechanics,” *Optics Express* **15**, 17172–17205 (2007).
- [58] Q. Rolland, M. Oudich, S. El-Jallal, S. Dupont, Y. Pennec, J. Gazalet, J. Kastelik, G. Lévêque, and B. Djafari-Rouhani, “Acousto-optic couplings in two-dimensional phoxonic crystal cavities,” *Applied Physics Letters* **101**, 061109 (2012).
- [59] M. Moccia, G. Castaldi, S. Savo, Y. Sato, and V. Galdi, “Independent manipulation of heat and electrical current via bifunctional metamaterials,” *Physical Review X* **4**, 021025 (2014).
- [60] C. Lan, K. Bi, X. Fu, B. Li, and J. Zhou, “Bifunctional metamaterials with simultaneous and independent manipulation of thermal and electric fields,” *Optics express* **24**, 23072–23080 (2016).